Materials Research, Vol. 6, No. 4, 445-449, 2003.

Er Rare-earth Ion Incorporation in Sol-Gel SnO_2

Evandro Augusto Morais[a], *Luis Vicente de Andrade Scalvi*[b]*, *Viviany Geraldo*[a], *Sidney José Lima Ribeiro*[c], *Celso Valentim Santilli*[c]

[a]*Instituto de Física de São Carlos - USP*
C.P. 369, 13560-970 São Carlos - SP, Brazil
[b]*Departamento de Física - FC - UNESP*
C.P. 473, 17033-360 Bauru - SP, Brazil
[c]*Instituto de Química Araraquara - UNESP*
C.P. 355, 14801-907 Araraquara - SP, Brazil

Received: January 29, 2003; Revised: June 30, 2003

Er-doped SnO_2 thin films and xerogels are obtained by sol-gel technique. In order to understand the Er^{3+} rare-earth ion activity in SnO_2 matrix, a characterization of Er incorporation is done through emission and excitation spectra of xerogels, besides thin film electrical characterization. Effects to grain dimensions are also analyzed based on X-ray diffraction data showing the particle growth with annealing temperature and inhibition of this growth by Er doping. Electrical characterization results suggest that Er^{3+} has an acceptor-like character in SnO_2, and that codoping with Yb^{3+} allows an energy transfer process $Yb^{3+} \rightarrow Er^{3+}$.

Keywords: *tin-dioxide, sol-gel, erbium, X-ray diffraction*

1. Introduction

In the last decades, rare-earth doped materials have been obtained widespread interest, since they can contribute for technological innovation. Rare-earth incorporation in semiconductors has many applications in optoelectronic devices. Er^{3+} ion presents several radiative transition concerning decay from several excited core levels to ground state, yielding emission from visible to infrared. Particularly the 4f transition about 1540 nm coincides with minimum absorption of fiber optics[1], being of great interest for optical communication. In the other hand, tin dioxide is a wide bandgap semiconductor (about 3.5-4.0 eV) [2], which has been widely applied due to its physical and chemical properties. SnO_2 thin films are characterized by high electrical conductivity and transparency about 80-90% in the visible and high reflectivity in the infrared[2]. Undoped SnO_2 is an n-type semiconductor since oxygen vacancies or interstitial Sn^{4+} are donor sites. In the case of sol-gel films, crystallites are rather small (3-10 nm) [3] and a lot of oxygen is adsorbed at boundary layer, trapping electrons from the conduction band[4]. Then conductivity can be greatly increased by eliminating oxygen from grain boundary layer, which can be done by annealing at proper temperature and gas composition of the annealing chamber[5]. Er^{3+} is expected to be an acceptor in SnO_2 since when it substitutes Sn^{4+} in the rutile SnO_2 structure, removes an electron from valence band, leaving a hole, which may recombine with a free electron.

The main goal of our investigation is doping a high transparency matrix with an attractive core transition ion, contributing for production of devices with high capacity of optical transmission, where there is low optical loss, and doping with optically active elements[6]. The first investigation of rare earth doping in SnO_2 concerns Eu and Tb[7-10]. Therefore some conclusions drawn in this paper refers to comparison to Eu-doped SnO_2.

Besides, in this work we present evidences of Er incorporation in SnO_2 xerogels and thin films, from emission and excitation spectra from xerogels and electrical characterization of thin films. X-ray diffraction data in function of annealing temperature are also presented, showing the influence of Er doping concentration for particle growth during heating procedure.

*e-mail: scalvi@fc.unesp.br
Trabalho apresentado no XV CBECIMAT, Natal - RN, Novembro de 2002.

2. Experimental

Colloidal suspensions have been prepared by sol-gel process[7]. To an aqueous solution 0.2 molar of $SnCl_4.5H_2O$ was added the desired amount of $ErCl_3.6H_2O$. Under magnetic stirring, NH_4OH was added until pH reaches 11. Then the suspension is submitted to dialysis with distilled water by 10 days in order to eliminate Cl^- and NH_4^+ ions. After conclusion of this process, the sol presents semitransparent aspect.

The xerogel is obtained by keeping the sol at rest, at room temperature by one week. Yb^{3+} adsorption is obtained by adding SnO_2:Er powder to an aqueous solution of $YbCl_3.6H_2O$, and waiting 24 h before washing with distilled water.

Thin films were prepared at room temperature upon deposition on a borosilicate substrate through dip-coating technique, with a withdrawing rate of 10 cm/min until 30 dips.

For experiments of emission and excitation, xerogels are annealed at 1000 °C by 6 h. For X-ray diffraction measurements, they are treated at different temperatures from 100 to 1000 °C. For emission and excitation spectra it was used a xenon lamp of 450 W, a SPEX F212I Fluorimeter and a Germanium detector. For X-ray diffraction measurements it was used a Rigaku diffractometer coupled with a Cu source of 40 kV and 20 mA of current. Detector rate is 3 degrees per minute with a 0.02-degree step. To electrical characterization of thin films, in electrodes are evaporated on the sample through a shadow mask in a Edwards evaporation system, and submitted to annealing at 150 °C by 20 min. In order to perform measurements in the range of 25 to 300 K we use an Air Products cryogenic chamber.

3. Results and Discussion

Figure 1 shows excitation spectra for SnO_2:4%Er and SnO_2:0.1%Er xerogels, keeping emission at 1530 nm, which corresponds to radiative transition from excited $^4I_{13/2}$ state to ground $^4I_{15/2}$ state. The inset in Fig. 1 is the emission spectra of SnO_2:4%Er under excitation at 328 nm. Curves in Fig. 1 are separated to better visualization. Besides slit opening is different and then, no comparison between intensities is possible. The obtained signal corresponds to best resolution allowed by our system. No significant difference in wavelength of observed bands is seen, which means that the spectra due to Er transitions are present in both cases. The most intense band takes place about 328 nm, corresponding to SnO_2 bandgap and related to electron-hole recombination. Er^{3+} intra-ff transitions are present, concerning the smaller peaks in Fig. 1, which states $^4F_{7/2}$, $^2H_{11/2}$, $^4S_{3/2}$ and $^4F_{9/2}$. On SnO_2 xerogel the intense SnO_2 forbidden gap transition suggests that Er^{3+} substitutes Sn^{4+} on cassiterite structure[11]. The inset in Fig. 1 shows peaks at 1512, 1525, 1543, 1562 and 1578 nm, which corresponds to Er^{3+} transitions of an ion located on a Sn^{4+} site in SnO_2 cassiterite structures[11]. All the features shown in Fig. 1 assure that Er is actually incorporated in the SnO_2 matrix. We have also observed an increase in luminescence of xerogels by introduction of Yb in codoped samples, which takes place due to an energy transfer process $Yb^{3+} \rightarrow Er^{3+}$. This process is shown to be effective since Er luminescence is obtained by pumping with 980 nm (Yb^{3+} transition)[12].

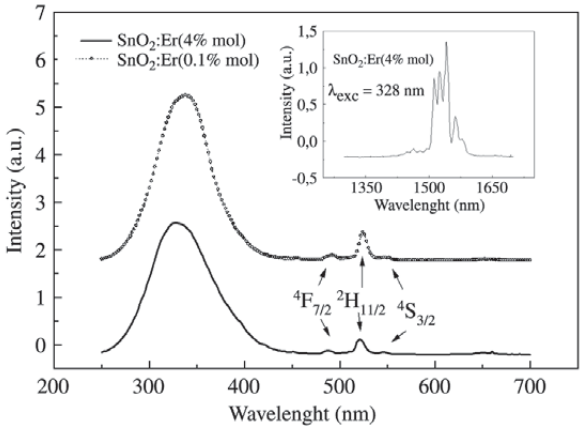

Figure 1. Excitation spectra for SnO_2+4%Er and SnO_2+0.1%Er xerogels, emission fixed at 1530 nm. Inset-Emission spectra for SnO_2+4%Er xerogel, excitation fixed at 328 nm.

Figure 2 shows resistivity as function of temperature for some thin films. The inset in Fig. 2 shows current-voltage experiments for SnO_2:2%Er above room temperature. Undoped SnO_2 has n-type conduction and, as seen in Fig. 2, much lower resistivity compared to Er-doped films. The increase in resistivity due to Er addition is probably related to acceptor -like behavior of Er^{3+} [13] in these films, leading to a high degree of compensation. The resistivity becomes so high that we can not measure it below 200 K for most samples due to equipment limitations. It is interesting to notice that the film SnO_2:4%Er behaves as SnO_2:0.1%Er, at low temperature, but with higher resistivity due to higher doping concentration. It is in good agreement with acceptor-like nature of Er. Then the higher the doping the more charge compensation there is in the film. Results shown in the inset of Fig. 2 may be related to dominant conduction mechanisms. A plot of $\ln j \times E^{1/2}$ (j - current density, E - applied electric field), not shown here, leads clearly to two distinct conduction mechanisms. For applied voltage until about 200 V the conduction is due to termionic emission over the grain potential barrier (Schottky mechanism) and for higher applied voltage the coulombic centers are ionized due to Poole-Frenkel conduction mechanism[14]. In the current-voltage curve, it means a non linear behavior,

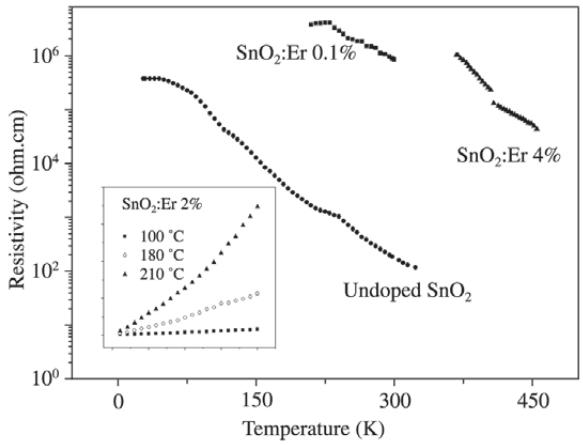

Figure 2. Resistivity as function of temperature for some Er-doped thin films. Inset-Current-voltage characteristics above room temperature for SnO_2:2%Er.

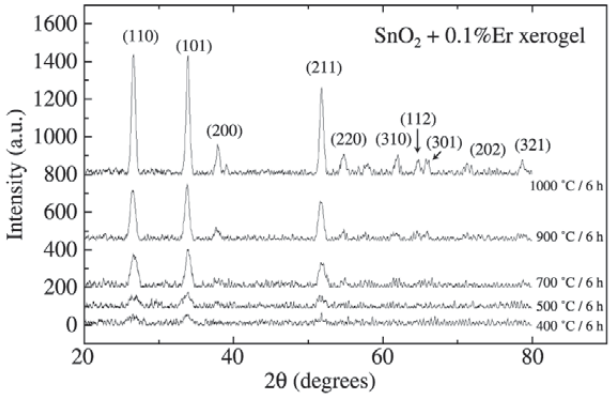

Figure 3. X-ray diffraction data for SnO_2+0.1%Er xerogel as function of annealing temperature. Lines separated for better visualization.

Table 1. Average particle size of SnO_2:0.1%Er xerogel.

Temperature (°C)	Direction (110) (nm)	Direction (101) (nm)
400	7.3	7.2
500	6.2	6.5
700	8.4	10.7
900	10.0	12.6
1000	13.2	16

which can be easily observed in the curve of the experiment carried out at 210 °C, shown in the inset of Fig. 2.

Figure 3 shows X-ray diffraction results to a SnO_2:0.1%Er xerogel under several annealing temperatures. It is clearly seen that the higher the annealing temperature, the lower the width and more intense are the diffraction peaks, which means that the crystallinity is increased. Comparing these results with cassiterite pattern[15], there is good agreement as indicated by crystal direction shown in Fig. 3. The average particle size (t) can be determined from diffraction peaks, using Scherrer[16] method, where t decreases with half width increase. The Scherrer equation is given by[16]:

$$t = \frac{K\lambda}{B\cos\theta}$$

where B is the broadening of half width at highest intensity and K is a constant, which is between 0.84 and 0.89, depending on geometry. B is evaluated considering contributions of broadening due to grain size and due to instrument broadening[16].

From diffraction peaks shown in Fig. 3, crystallite size has been evaluated, which is shown in Table 1. Only (110) and (101) directions are taken into account, since they present the highest intensity in X-ray diffraction pattern of SnO_2, being (110) the dominant[17]. Then these directions are good enough to allow an interpretation of diffraction spectra concerning evolution of crystallite dimensions. Particle size increases from 7.3 to 13.2 nm on (110) direction and a larger increase is observed for (101) direction, from 7.2 to 16 nm. This new crystallite dimensions means that there is a significant increase on material crystalinity.

Figure 4 shows the same kind of approach to a SnO_2:4%Er xerogel for some different annealing temperatures. Crystallite size evaluated from these results is shown in Table 2. Although there is also an increase in the crystallite dimension with annealing temperatures, the particle size is smaller than those obtained by the same treatment on SnO_2:0.1%Er. This result suggests that incorporation of Er impurity controls the grain growth. This dependency of particle size with Er^{3+} doping concentration is in good agreement with Eu^{3+}-doped SnO_2, since the excess of Eu^{3+} ions segregates at particle surface and retards crystallization compared to undoped xerogels[18]. Another important feature for this xerogel is that as the temperature is increased, there is a much larger growth on crystallite size on direction (110) than (101), which suggests a exchange on preferential direction for growth from (101) to (110), which is in good agreement with Lantto *et al.*[17], that state that in polycrystalline samples the [110] surface is the most perfect and stable. Strikingly this was not observed for SnO_2:0.1% Er. Although it is seen in Fig. 3 an exchange in intensity, the crystallite size increases much more in (101) direction than (110) direction.

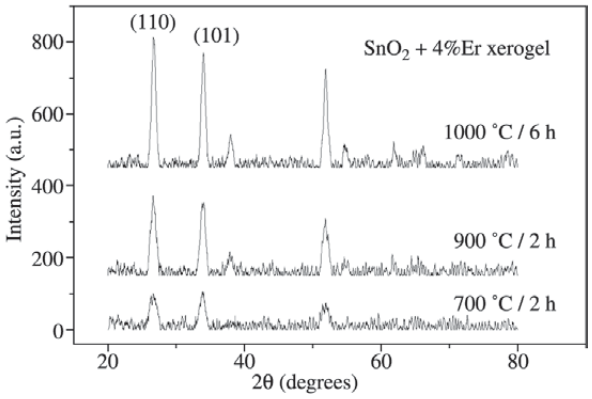

Figure 4. X-ray diffraction data for SnO_2+4%Er xerogel as function of annealing temperature. Lines are separated for better visualization.

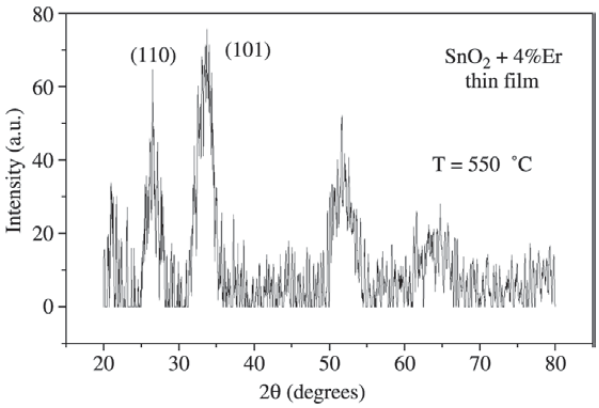

Figure 5. X-ray diffraction data for SnO_2:4%Er thin film treated at 550 °C.

Table 2. Average particle size of SnO_2:4%Er xerogel.

Temperature (°C)	Direction (110) (nm)	Direction (101) (nm)
700	6.2	8.7
900	8.7	9.2
1000	10.7	11.2

For comparison, we show in Fig. 5 a plot of X-ray diffraction results for a SnO_2:4%Er thin film, which has been treated at 550 °C. Scherrer equation applied to this result, yields an average grain size of 3.9 and 3.5 nm in the (110) and (101) directions, respectively. All the results of evaluation of grain size for the xerogel yields grains size higher than for thin film. Such a smaller grain size may contribute to increase the grain boundary scattering and, thus, to the observed high resistivity of these films, in conjunction with Er acceptor-like nature.

4. Conclusion

Excitation and emission spectra shows the incorporation of Er^{3+} in SnO_2 xerogel matrix. Keeping emission fixed at 1530 nm, no band shift on excitation spectra is observed upon increase in doping concentration. Emission spectra under excitation at 328 nm shows several peaks from 1520 to 1580 nm, corresponding to Er^{3+} core transitions, characteristic of a Er^{3+} located at Sn^{4+} on SnO_2 structure. Electrical characterization of SnO_2 thin films suggests the acceptor like character of Er impurity which leaves the SnO_2 matrix practically insulating.

Increasing the annealing temperature, the powder crystallization becomes quite clear, since particle size increases sharply, as evaluated from X-ray diffraction data. Incorporation of Er into SnO_2 xerogel inhibits the crystallite growth. Investigation of influence of co-doping with Yb^{3+} is under progress and the first results, showing the energy transfer process from Yb^{3+} to Er^{3+} are being published elsewhere[12].

Acknowledgments

The authors wish to thank Prof. Ligia O. Ruggiero for the help with the technical set-up, and CAPES, FAPESP, CNPq and MCT - PRONEX for the financial resources.

References

1. Coffa, S.; Franzó, G.; Priolo, F.; Polman, A.; Serna, R. *Phys. Rev. B*, v. 49, p. 16313, 1994.
2. Ray, S.C.; Karanjai, M.K.; Dasgupta, D. *Surface & Coatings Technol.*, v. 102, p. 73, 1998.
3. Souza, A.E.; Monteiro, S.H.; Santilli, C.V.; Pulcinelli, S.H. *J. Mater. Sci. Mater. Electron.*, v. 8, p. 265, 1997.
4. Messias, F.R.; Scalvi, L.V.A.; Siu Li, M.; Santilli, C.V.; Pulcinelli, S.H. *Rad. Eff. & Def. Solids*, v. 146, p. 199, 1999.
5. Messias, F.R.; Vega, B.A.V.; Scalvi, L.V.A.; Siu Li, M.; Santilli, C.V.; Pulcinelli, S.H., *J. Non-Crystalline Solids*, v. 247, p. 171, 1999.
6. Gonçalves, R.R.; Ferrari, M.; Chiasera, A.; Montagna, M.; Morais, E.A.; Scalvi, L.V.A; Santilli, C.V.; Messaddeq, Y.; Ribeiro, S.J.L. *J. Metastable and Nanocrystalline Materials*, v. 14, p. 107, 2002.
7. Ribeiro, S.J.L.; Pulcinelli, S.H.; Santilli, C.V. *Chem. Phys. Lett.*, v. 190, p. 64, 1992.
8. Ribeiro, S.J.L.; Hiratsuka, R.S.; Massabni, A.M.G.; Davolos, M.R.; Santilli, C.V. *J. Non-Crystalline Solids*, v. 147&148, p. 162, 1992.

9. Kynev, K.; Gutzov, S.; Peneva, S.K.; Apostolov, A.A. *Cryst. Res. Technol.*, v. 30, p. 281, 1995.
10. Zupanc Meznar, L.; Pracek, B.; Orel, B.; Bukocek, P. *Thin Solid Films*, v. 317, p. 336, 1998.
11. Ribeiro, S.J.L.; Santilli, C.V.; Pulcinelli, S.H.; Fortes, F.L.; Oliveira, L.F.C. *J. Sol-Gel Sci. Technol.*, v. 2, p. 263, 1994.
12. Morais, E.A.; Ribeiro, S.J.L.; Scalvi, L.V.A.; Santilli, C.V.; Ruggiero, L. O.; Pulcinelli, S.H.; Messadeq, Y. *J. Alloys and Comp.*, v. 344, p. 217, 2002.
13. Matsuoka, T.; Tohda, T.; Nitta, T. *J. Electrochem. Soc*., v. 130, p. 417, 1983.
14. Chang, J.P.; Lin, Y.S. *Appl. Phys. Lett.*, v. 79, p. 3666, 2001.
15. Powder Diffraction File, Inorganic v. 21, Publ. By the JCPDS, Swathmore, 1983.
16. Cullity, B.D. *Elements of X-ray Diffraction*, Addison-Wesley Pub. Comp., Massachusetts, 1978.
17. Lantto, V.; Rantala, T.T.; Rantala, T.S. *J. European Ceramic Society*, v. 21, p. 1961, 2001.
18. Britto, C.E.S.; Ribeiro, S.J.L.; Briois, V.; Dexpert-Ghys, J.; Santilli, C.V.; Pulcinelli, S.H. *J. Sol-Gel Sci. Technol*., v. 8, p. 261, 1997.